Measurements of the complex dielectric constant of volcanic ash from 4 to 19 GHz

R. J. Adams,[1] W. F. Perger,[2] W. I. Rose,[3] and A. Kostinski[4]

Abstract

Dielectric data in volcanic ash at weather radar wavelengths (centimeter range) are extremely sparse and are crucial for radar sensing of ash clouds and for imaging of volcanic terrains. This study extends previous data to include a wavelength range of 1.5-7.5 cm and volcanic ash compositions of 50-75 % silica. The real part of the complex permittivity, ϵ', of volcanic ash is 6 ± 0.5 (1σ) for all wavelengths. The imaginary part, ϵ'', ranges from 0.08 to 0.27. Both ϵ' and ϵ'' show higher values at lower SiO_2 concentration. It is safe to assume in any weather radar applications that the reflectivity factor is $K = |(\epsilon - 1)/(\epsilon + 2)|^2 = 0.39 \pm 0.02$ (1σ), regardless of composition or wavelength. The results will help quantify radar observations of volcanic clouds.

[1]ElectroMagnetic Interactions Laboratory, Bradley Department of Electrical Engineering, Virginia Polytechnic Institute and State University, Blacksburg, VA 24061-0111

[2]Departments of Electrical Engineering and Physics, Michigan Technological University, Houghton, MI 49931-1295

[3]Department of Geological Engineering and Sciences, Michigan Technological University, Houghton, MI 49931-1295

[4]Department of Physics, Michigan Technological University, Houghton, MI 49931-1295

Introduction

The use of radar and microwave instruments for sensing volcanic phenomena has particular value in regions of frequent activity, remote locations, and cloudy weather. Development of their remote sensing potential is part of an interdisciplinary science team focusing on volcanos for NASA's Earth Observing System [*Mouginis-Mark et. al*, 1991]. The impetus for the present research comes from the paucity of data on the dielectric constants of volcanic ash. Only one reference with specific data [*Campbell and Ulrichs*, 1969] has been located, and that study offered results on only two samples at two specific wavelengths, 450 MHz and 35 GHz. There is therefore an urgent need for data over a wide range of wavelengths and for a variety of ash compositions. These data are needed for two applications of remote sensing: one which senses eruption columns and clouds in the atmosphere with meteorological radar systems [*Harris and Rose*, 1983, *Rose and Kostinski*, 1994] and another which uses imaging radar (e.g., the recent Shuttle Imaging Radar (SIR-C) mission) to sense and map volcanic ash deposits on the ground, including volcanic ashfalls, ash flows, mudflows, and lavas. Note that the former application requires a dielectric constant of a solid rock equivalent of a dilute volcanic ash suspended in air (in order to compute the radar backscattering cross - section), while the latter requires an effective dielectric constant of a dense volcanic ash powder on the ground (viewed as a rough surface). To obtain an effective dielectric constant, we report using a microwave technique which involves placing a quantity of volcanic ash in a shorted waveguide. The standing wave which results will have its nulls shifted, which is more - or - less a consequence of the real part of the complex dielectric constant of the ash. The ratio of the maximum electric field to the minimum (the standing wave ratio) will decrease as a result of the presence of losses in the ash, which is a consequence of the imaginary part of the complex dielectric constant.

The dielectric constant is a measure of the polarizability of a material. When an electric field is impressed on a material with intrinsic, microscopic dipoles (a "ball and stick" model will suffice as a simple but incomplete picture), the dipoles will realign so as to modify the total electric field. That is, the total electric field will now be the sum of the impressed electric field and the electric field of the dipoles. This is generally expressed through the constitutive relation:

$$\vec{\mathbf{D}} = \epsilon_r \epsilon_o \vec{\mathbf{E}}. \tag{1}$$

One of Maxwell's equations in time-harmonic form is

$$\nabla \times \vec{\mathbf{H}} = \vec{\mathbf{J}} + j\omega\epsilon_r\epsilon_o\vec{\mathbf{E}}, \tag{2}$$

where $\vec{\mathbf{J}} = \sigma\vec{\mathbf{E}}$ in equation (2) is the conduction current. Combining equations (1) and (2) results in the definition of an effective complex relative permittivity, ϵ:

$$\nabla \times \vec{\mathbf{H}} = j\omega\epsilon\epsilon_o\vec{\mathbf{E}}, \tag{3}$$

where $\epsilon = \epsilon' - j\epsilon'' = \epsilon_r - j\left(\sigma/\left(\epsilon_o\omega\right)\right)$. The ratio ϵ''/ϵ' is commonly referred to as the loss tangent, and $j = \sqrt{-1}$ (note that we are using the choice of j and not i for $\sqrt{-1}$, as is commonly done in electrical engineering literature).

We chose to work on volcanic ash materials, rather than with solid rock, for two reasons. First, we wanted to use ash samples from a variety of recent eruptions which have been extensively studied, and it was difficult to get solid rock compositional equivalents of all of these materials. Volcanic ash is subject to atmospheric fractionation and has complex shapes and many voids (vesicles). Second, we wanted to be able to address the dielectric properties of ash that has fallen on the ground as a fairly dense aggregate of sand, silt, or clay-sized particles, as well as dilute suspended particles in the atmosphere, with the same set of laboratory experiments.

Dense ash powder is a mixture of a solid material and air, and it is the effective dielectric constant of this mixture which is measured. One then has to use appropriate mixing formulae to recover the solid ash dielectric constant which is needed in radar scattering calculations (e.g., eruption monitoring). The volume fraction of ash was determined from a measurement of the sample mass and a knowledge of the sample density. As we show below, the results obtained from the powder measurements and appropriate mixing formulae agreed with those obtained directly from a solid sample. In addition, from such comparisons one can learn about the validity of various mixing formulae for volcanic ash and thereby make some inferences about shape, etc.

The structure of this article will be an overview of the experimental method used, followed by a presentation of the complex permittivity values determined for the ash samples listed in Table 1. The important issues of error analysis and the choice of an appropriate mixing formula are included as appendices in order to highlight the results while also providing the

details necessary for a critical analysis of the methodology.

Measurement Technique and Apparatus

All measurements of the complex permittivity were made using a short-circuited slotted rectangular wave guide operating in the TE_{10} mode (the TE_{10} mode is the "transverse electric" mode with one half cycle in the direction of the width of the guide and constant along the direction of the height of the guide). Since the complex permittivity ($\epsilon = \epsilon' - j\epsilon''$) is not a directly measurable quantity, it is necessary to relate ϵ to the physically measurable parameters in the experiment. This is accomplished by equating two expressions for the waveguide's characteristic impedance at the air-sample interface (the impedance is the ratio of the transverse electric to the transverse magnetic field). Looking from medium 1 (air) to medium 2 (ash), with medium 2 terminated by an electrically shorting plate (see Figure 1), the characteristic impedance is given by the relation [*Westphal*, 1954, p. 66]

$$Z(0) = Z_2 \ \tanh\,(k_2 d), \tag{4}$$

where d is the sample thickness and Z_2 and $k_2 = jk_2' + k_2''$ are the complex characteristic impedance and complex wave number within the sample, respectively. For nonmagnetic materials (where the permeabilities, μ_1 and μ_2, are identical), we may substitute $Z_2 = Z_1 k_1/k_2$ in equation (4) to obtain

$$Z(0) = Z_1(k_1/k_2) \ \tanh\,(k_2 d), \tag{5}$$

where Z_1 and k_1 are the complex characteristic impedance and wavenumber in region 1 (the free-space region of the waveguide).

Similarly, looking from medium 2 to medium 1, *Westphal* [1954, p. 66] showed that

$$Z(0) = Z_1 \frac{\frac{E_{\min}}{E_{\max}} - j\tan\left(\frac{2\pi x_o}{\lambda_1}\right)}{1 - j\frac{E_{\min}}{E_{\max}}\tan\left(\frac{2\pi x_o}{\lambda_1}\right)}. \tag{6}$$

Here $E_{\min}/E_{\max}$ is the inverse of the standing wave ratio (SWR), λ_1 is the wavelength in the air-filled guide, and x_o is the distance from the air-sample interface to a minimum in the standing wave pattern.

Equating equations (5) and (6) and recognizing that $k_1 = j2\pi/\lambda_1$, an expression for the unknown complex characteristic wave number k_2 is obtained in terms of measurable parameters:

$$\frac{\tanh\,(k_2 d)}{k_2 d} = \frac{-j\lambda_1}{2\pi d}\left(\frac{\frac{E_{\min}}{E_{\max}} - j\tan\left(\frac{2\pi x_o}{\lambda_1}\right)}{1 - j\frac{E_{\min}}{E_{\max}}\tan\left(\frac{2\pi x_o}{\lambda_1}\right)}\right). \tag{7}$$

The right side of equation (7) is completely in terms of measurable parameters. Assuming TE_{10} mode propagation, λ_1 is determined by a simple measurement of the standing wave pattern in the guide for a short-circuited load with no sample. The quantities x_o and $E_{\min}/E_{\max}$ are found from measurements on the slotted line using a simple square - law detector. Once k_2 has been determined, the complex relative permittivity for nonmagnetic materials is found as

$$\epsilon_2 = \frac{\left(\frac{1}{\lambda_c}\right)^2 - \left(\frac{k_2}{2\pi}\right)^2}{\left(\frac{1}{\lambda_c}\right)^2 + \left(\frac{1}{\lambda_1}\right)^2}, \tag{8}$$

where λ_c is the cutoff wavelength.

The determination of the right-hand side of equation (7) in terms of measurable parameters does not uniquely define k_2. This ambiguity results because the impedance has only been defined at the sample boundaries. It is therefore necessary to determine which of the infinite number of solutions to the transcendental equation (7) is correct. This can be effectively accomplished by choosing the depth of the sample holder d sufficiently small.

Neglecting losses, equation (7) simplifies to (cf. equation (A2))

$$\tan\,(k_2' d) = k_2' \xi_{\exp}, \tag{9}$$

where $\xi_{\exp}$ is an experimentally determined constant which is implicitly dependent upon both k_2' and d. As this equation indicates, the spacing between the discrete values of k_2 which satisfy equation (9) can be increased by choosing d smaller. For d sufficiently small, this allows the solutions to equation (7) which are adjacent to the correct value to be discarded on a physical basis. Consider the simplest case for which $\xi_{\exp}$=0. Then equation (9) is satisfied for

$$k_2' = \frac{n\pi}{d} \tag{10}$$

where n is an integer. Thus, when d is large, the solutions k_2' are closely spaced, while for small values of d, the solutions become widely separated.

For example, the following four adjacent solutions to equation (7) were obtained for the ash sample 2567

at 10 and 13 GHz in the X-band guide using a sample holder with $d = 1.78$ cm:

$$\epsilon_{10} = \begin{cases} 1.05 - j0.008 \\ 2.90 - j0.028 \\ 6.02 - j0.050 \\ 10.5 - j0.075 \end{cases} \quad \epsilon_{13} = \begin{cases} 1.21 - j0.031 \\ 2.90 - j0.031 \\ 5.41 - j0.031 \\ 8.78 - j0.031 \end{cases} .$$

Assuming a constant permittivity for sample 2567 between these two frequencies, the only solution which satisfies both the 10- and 13-GHz cases within experimental error is $\epsilon = 2.9 - j0.03$. Other roots may be available which also satisfy both cases, but they must be outside the range of values listed above and are therefore not physically reasonable.

Solutions to the multivalued, transcendental equation (7) were obtained using a root-finding algorithm in the commercial symbolic math package Mathematica [*Wolfram*, 1989].

The short-circuited waveguide technique was used to measure the permittivity of all ash samples. While it is possible to measure both the permittivity and permeability of a sample using the shorted waveguide technique, all of the ash samples measured have a small magnetic material content, and it has been assumed that the samples are nonmagnetic ($\mu = \mu_0$). This is the same assumption made by *Campbell and Ulrichs* [1969] when making similar measurements and results in a loss tangent which includes both electric and magnetic field losses.

Commercial slotted guides with cutoff frequencies of 6.6 and 9.6 GHz were used to make measurements from 7 to 19 GHz (X - and Ku - bands, respectively). From 3.5 to 6 GHz (C - band), measurements were made using a waveguide with a cutoff of 3.1 GHz with a machined slot. The sample holders were constructed by welding copper plates to one end of short sections of the waveguide. These sample holders ranged in length from 1.8 to 2.5 cm.

The slotted section of waveguide and the ash samples were mounted vertically so that additional containers were not required to hold the powdered samples in place. All samples were dried in an evacuated oven for 8 hours at 110 °C and allowed to cool to room temperature before measurements were taken. The ash samples were then prepared by packing the powdered ash into the short-circuited sections of waveguide. Excess ash was scraped off to produce a sample surface which was flush with the waveguide flange. The fractional volume of the powdered samples, defined as

$$f_\nu = \frac{M/V}{\rho}, \tag{11}$$

where M is the mass, V the volume, and ρ the density, varied from 0.43 to 0.63. However, the fractional volume of each individual ash sample split varied less than 3.5% from the mean (a split is defined as one of several sub-specimens of a given sample).

Effective Permittivity of Powdered Ash Samples

The real and imaginary parts of the complex dielectric constant of the samples listed in Table 1 were measured in the frequency range 4-19 GHz using the technique discussed above. The real and imaginary parts of the complex permittivity for a representative sample, VF74-148, are plotted as a function of frequency in Figures 2 and 3, respectively. Notice that along with the expected variation of the measured permittivity for a given split (discussed in Appendix A), the measured permittivity values of the sample also exhibit a split-to-split variation.

This variation is attributed to two distinct effects. The first is deterministic in nature and arises due to variations in the volume fraction for different splits (see Figure 4). This effect is removed in determining the solid ash permittivity through the use of an appropriate mixing formula (see Appendix B). The second reason for the split-to-split variation observed in Figures 2 and 3 is the stochastic nature of the problem. The effective permittivity of each split is a complicated function of the size, shape, location, orientation, permittivity, and volume fraction of the particles in the specimen. Thus, even for splits with identical volume fractions, the effective permittivity is a random variable and must be statistically described by its moments over several splits.

The mean and standard deviation of the measured relative permittivity of the powdered ash samples are listed in Table 2. These numbers were obtained by averaging all measurements of a given sample over all splits and all frequencies. It should be noted, as discussed in Appendix A, that only one of the samples (SM-3) exhibited a measurable variation in its relative permittivity with frequency. A variation of approximately $+j0.004$ GHz^{-1} was observed in the imaginary portion of the relative permittivity of this sample. The corresponding variation in the real part of the permittivity (as required by the Kramers-Kronig relations) was not measurable.

Calculated Permittivity of Volcanic Ash (Using Böttcher's Formula)

The real and imaginary relative permittivities of the solid ash for all six ash samples are shown in Table 2. These values were obtained by using Böttcher's formula to relate the average effective permittivity, ϵ_{eff}, and average volume fraction, f_v, to the desired solid ash permittivity, ϵ_s (see Appendix B for a discussion of the formula). The formula was applied to the average permittivities over all splits rather than to the permittivity values determined from the individual splits because ϵ_{eff} in equation (B1) is, by definition, an average quantity and cannot be determined from a single measurement of a sample. The average value of f_v for a given sample was also used in obtaining the values listed in Table 2, and although (B1) is nonlinear with respect to the volume fraction, the variation of f_v for a given sample was small (Table 3) and the error due to this linearization has been neglected.

Concluding Remarks

The measurements made of the real and imaginary parts of the complex dielectric constant of powdered volcanic ash samples indicate that to within experimental uncertainty, these parameters are essentially independent of frequency in the C -, X - and Ku - bands.

A linear relationship between the chemical composition of volcanic ash and the ash permittivity has been identified (Figure 5) for the ash samples considered herein. Both the real and imaginary parts are slightly higher (∼10-20%) for ash with lower silica contents.

Our new data are comparable and in basic agreement with results reported by *Campbell and Ulrichs* [1969] for whole rock samples at 450 MHz and 35 GHz. Their results for Newberry Obsidian were 5.5 and 5.4, respectively, which is very close to our value for rhyolitic ash (sample 2567, $\epsilon' = 5.649$). Campbell and Ulrichs included in their paper results from rocks which are called "pumice," "tuff," and "volcanic ash," which had lower permittivities (2.5-4.0). We suspect these samples had a significant porosity and would have dense rock equivalent permittivities of about 5.5-6.5.

All weather radars operate in the wavelength range of 3-10 cm (with National Weather Service systems at 10 cm). In this study, we covered the range of 1.5-7.5 cm with $\epsilon' = 6 \pm 0.5$ and ϵ'' =0.08-0.27 throughout the range. What matters in scattering applications is the radar cross - section, σ, which is proportional to [*Ishimaru*, 1991]

$$K = \left| \frac{\epsilon - 1}{\epsilon + 2} \right|^2 , \tag{12}$$

where the vertical bars denote the absolute value and K is usually referred to as the reflectivity factor. Substituting ϵ' and ϵ'' values quoted above, we obtain $K = 0.39 \pm 0.02$ ($\pm 1\sigma$). Thus we conclude that in any weather radar application, the reflectivity factor is $K = 0.39 \pm 0.02$ ($\pm 1\sigma$), regardless of composition or wavelength.

The reflectivity factor is used to determine the intensity of radar reflections. By comparison, this factor is 0.93 for water and 0.197 for ice, and we note that at the same size and wavelength, ash is a factor of 2.4 less reflective than liquid water and 2 times more reflective than ice. These data show why moisture content of volcanic ash on the ground will be the dominant factor in its scattering.

Appendix A: Calibration and Error Analysis

The scales on the slotted waveguides were capable of measuring a ±0.01-cm shift in the position of the standing wave. The length of the sample holders was measurable to ±0.015 cm. The inverse SWR was measurable to ±0.25 dB at Ku - band using a variable attenuator. At C - and X - band, the double minimum technique was used to measure the inverse SWR to $\pm 0 - 2$ dB, with the measurement accuracy dependent upon the sample's loss tangent and the fraction of a wavelength contained within the sample [*Westphal*, 1954, p. 67]. Finally, the cutoff and actual wavelength at each frequency (λ_c and λ_1) were measurable to within ±0.005 cm.

Given these values, it is possible to use equations (7) and (8) to bound the errors in determining ϵ_2' and ϵ_2'' which are due to measurement uncertainties. Furthermore, because the ash samples we are considering have small loss tangents (ϵ''/ϵ'), it is possible to estimate the sensitivity of the real portion of the dielectric constant to the experimental parameters independently of ϵ''. This is because to first order,

$$\omega\sqrt{\mu_o\epsilon_2} = \omega\sqrt{\mu_o}\sqrt{\epsilon_2' - j\epsilon_2''} \approx \omega\sqrt{\mu_o\epsilon_2'}\left(1 - j\frac{\epsilon_2''}{2\epsilon_2'}\right) \tag{A1}$$

and the phase shift (i.e., shift in null location) is independent of ϵ_2'' (the subscript 2 refers to region 2). The inverse is not true, however, and the measured value of ϵ_2'' is dependent upon both the measured SWR and null location.

Error in Determining ϵ_2'

Assuming the inverse SWR is zero, equation (7) reduces to

$$\frac{\tan\,(k_2' d)}{k_2'} = \frac{-\lambda_1}{2\pi} \tan\left(\frac{2\pi x_0}{\lambda_1}\right), \qquad \text{(A2)}$$

where k_2' is real. Because the measurement uncertainties are much smaller than a wavelength, the error in determining k_2' can be bounded as [*Bevington*, 1969]

$$\begin{aligned} \Delta k_2' \quad \leq \quad & \left|\Delta x_o \frac{\partial k_2'}{\partial x_o}\right| + \left|\Delta d \frac{\partial k_2'}{\partial d}\right| + \left|\Delta \lambda_1 \frac{\partial k_2'}{\partial \lambda_1}\right| \\ & + \left|\Delta \lambda_c \frac{\partial k_2'}{\partial \lambda_c}\right|. \end{aligned} \qquad \text{(A3)}$$

Using this result along with equation (8), the error in determining ϵ_2' satisfies

$$\Delta\epsilon_2' \leq \left|\Delta k_2 \frac{\partial \epsilon_2'}{\partial k_2}\right| + \left|\Delta \lambda_1 \frac{\partial \epsilon_2'}{\partial \lambda_1}\right| + \left|\Delta \lambda_c \frac{\partial \epsilon_2'}{\partial \lambda_c}\right|. \qquad \text{(A4)}$$

Equation (A4) is the desired result which bounds the maximum deviation of ϵ_2' due to errors in determining the various parameters in the experiment. However, this bound will generally be different for each different dielectric constant measured at a given frequency. In addition, equations (A3) and (A4) require that we know the correct values of k_2' and ϵ_2', while the experiment only estimates these values. Thus direct application of (A4) to the experimental data results in an error bound on the variation of the (generally imprecisely known) measured dielectric constant, not the desired bound on the variation of the measurements from the actual dielectric constant.

An acceptable solution to these problems was obtained by numerically determining the maximum fractional error in each of the three frequency bands over the range of dielectric constants encountered in the experiment (ϵ_2' =2.5-3.8). The fractional error is defined as

$$f_{\text{err}} = \frac{2\Delta\epsilon_2'}{\epsilon_2'} \qquad \text{(A5)}$$

where $\Delta\epsilon_2'$ is obtained using (A4). It should be noted that in performing these numerical calculations, the singularities of (A2) (i.e., when $x_o/\lambda_1 = (2n+1)\pi/4$) do not present a problem. Although a small change in x_o near these singularities can lead to a large change in the right side of (A2), the left side exhibits a similar singularity, and the error predicted by (A4) is a smoothly varying function for all parameter combinations. This ensures that there are no highly localized parameter combinations that produce very large errors which might be missed in a numerical calculation designed to bound the error.

The maximum fractional errors (f_{err}) produced by these numerical calculations were 0.046, 0.084, and 0.080 at C -, X -, and Ku - bands, respectively. One-half of these values multiplied by 100 yields the maximum percentage error in determining ϵ_2'. The value f_{err} is used here so that comparisons can be made with the experimental data for which the mean is not known. As shown in Table A1, although the ash splits consisted of randomly situated scatterers, not a continuous dielectric as assumed in the development of equations (7) and (8), the variation observed in the actual measurements was significantly smaller than the numerically determined bounds given above. This implies that the variation of our measurements of ϵ_2' from the true mean is conservatively bounded in all cases by 4.2%.

Finally, to check the above error analysis, permittivity measurements were made of Teflon using the Ku-band guide. Teflon has a constant relative permittivity of $2.08 - j10^{-4}$ in the frequency range considered here [*von Hippel*, 1954, p. 322]. More recent measurements of the permittivity of Teflon were made using a time domain measurement of S - parameters and show the real part to be about 2.06 at 2.9 GHz, dropping monotonically to 2.01 at 11.7 GHz [*Hewlett-Packard Corporation*, 1985]. Our measured values therefore are within the experimental uncertainty of our apparatus, as shown in Figure A1, which illustrates the variation of the measurements made on a sample of Teflon at Ku - band along with the value cited by *von Hippel* [1954]. Maximum errors of 1.8 and 4.7% are obtained when compared with the values cited by *Hewlett-Packard Corporation* [1985] and *von Hippel* [1954], respectively, and the maximum fractional variation across the range is 0.017.

Error in Determining ϵ_2''

The maximum error in determining ϵ_2'' due to measurement uncertainties can be determined using a procedure similar to that illustrated above for ϵ_2'. However, we must now use equation (7) instead of (A2). In

addition, small deviations from the ideal TE_{10} model due to the nonideal nature of the problem become more important in determining the errors in ϵ_2''. This is because the loss tangents of some of the ash samples are small, and these secondary effects in the nonideal waveguide can produce field strengths which, at the nulls of the standing wave pattern, are significant compared with those which are due to the propagation of the TE_{10} mode.

Assuming ideal TE_{10} propagation and a maximum error in determining the inverse SWR, E_r, of ± 0.25 dB yields maximum expected fractional errors of 0.13, 0.26, and 0.40 at C -, X -, and Ku - band, respectively. However, as mentioned above, the error in determining E_r at C - and X - band was a function of the standing wave ratio and varied from ± 0 to 2 dB. Assuming an error of ± 1 dB at C - and X - bands yields maximum expected fractional errors of 0.30 and 0.42, respectively.

Table A2 shows the variation of ϵ_2''. Notice that the maximum deviation is generally larger for the samples with smaller loss tangents (cf. Table 2). In some instances the variation exceeds the above predicted bounds on the variation in these parameters. This is reasonable, since when the field strength at a null in the standing wave is small, the instrument is more likely to respond to weak nonidealities in the guide which are not included in the simple TE_{10} model. The effect these nonidealities have on the data can be lessened by taking advantage of the manner in which E_r varies with frequency (see Figure A2). For the apparatus and samples used in this experiment, it was found that data points for which $E_r < -25$ dB exhibited large variations from the mean. Therefore, in determining ϵ_2'', only those measurements for which E_r exceeded -25 dB were used.

Given this restriction, the maximum error in determining E_r is ± 1 dB for C - and X - band measurements, and the maximum expected fractional variation at C -, X -, and Ku - bands is 0.30, 0.42, and 0.40, respectively. The maximum observed variation of the measurements for which $E_r > -25$ dB is shown in Table A3. Those entries indicated with a 0 correspond to trials for which only one measurement satisfied $E_r > -25$ dB. In virtually all cases, the variation is significantly less than when all the data points are used (cf. Table A2). For all but one sample, the maximum measured variation is well within the predicted bounds. This sample (SM-3) exhibits a large variation in ϵ_2'' because it has a significant positive slope in ϵ_2'' across the frequencies being considered. Although this slope was measurable, it has been explicitly ignored in the calculation of the average quantities $< \epsilon'' >$ and $< \epsilon''_{\text{eff}} >$. The slope is effectively included, however, through a resultant increase in the standard deviation of ϵ_2'' for this sample (see Table 2).

Appendix B: Mixing Formulae

In order to determine the actual permittivity of the solid volcanic ash, a mixing formula must be used to relate the permittivity and porosity of the ash and air mixture to a specific solid ash value (the quasi-static limit is assumed, since $d \ll \lambda$ for all ash samples). The literature contains a large number of mixing formulae dating from as early as 1821 [*van Beek*, 1967], but little experimental data other than that of *Campbell and Ulrichs* [1969] has been found which evaluates the accuracy of these formulae for complex substances such as rocks and volcanic ash. The formulae which are applicable to our problem give significantly different values for the solid - ash permittivity.

In addressing this same problem at 450 MHz, *Campbell and Ulrichs* [1969] found strong experimental support for the use of Rayleigh's mixing formula on mixtures with fractional volumes of up to approximately 60%. However, the Rayleigh formula assumes that the field in the region of an individual particle in the mixture is not perturbed by neighboring particles and thus requires $f_\nu \ll 1$ ([*van Beek*, 1967] suggests $f_\nu \ll 0.2$). Application of the Rayleigh formula to our data gives unrealistic values for the solid ash permittivity values, and we have investigated the use of other mixing formulae.

The accuracy of five different mixing formulae was examined by measuring the solid and powdered permittivity values of three different rock samples (Table B1). Measurements were made by cutting and polishing portions of three different solid rock samples to fit in the C-band sample holder. The remaining portions of the original rock were then shattered to obtain the powdered rock permittivity measurements. The particle sizes of the crushed rock sample were similar to the particle sizes of the ash samples under consideration. The mixing formulae listed in Table B1 are given by *van Beek* [1967].

For a given volume fraction of powder, which mixing formulae is most appropriate depends on, among others, the relative permittivity of the sample being measured (Table B1). As is also seen in Table B1 and discussed by *Ulaby* [1986, p. 2085], the solid - rock dielectric constant is related to the

rock's density. Therefore, because the range of ash sample densities measured here (2.5-2.7 g/cm^3) includes the density of the granite sample in Table B1, for which Böttcher's formula accurately relates the solid and powdered granite permittivities, we have applied Böttcher's mixing formula to our data. We have chosen Böttcher's formula over Looyenga's mixing formula because both performed similarly and Böttcher's formula is more familiar.

Böttcher's formula implicitly expresses the measured effective permittivity of a mixture of spherical particles as a function of the background (ϵ_b) and inclusion (ϵ_s) permittivities:

$$\frac{\epsilon_{\text{eff}} - \epsilon_b}{3\epsilon_{\text{eff}}} = f_v \frac{\epsilon_s - \epsilon_b}{\epsilon_s + 2\epsilon_{\text{eff}}}. \tag{B1}$$

This expression, also known as the Polder-van Santen mixing formula for spherical particles [*Polder and van Santern*, 1946], has been derived using various techniques by several authors [*Böttcher and Bordewijk*, 1978, *Polder and van Santern*, 1946, *Tsang and Kong*, 1981, *Taylor*, 1965]. In arriving at this formula, it is assumed that the mean field inside a particle surrounded by the effective medium (ϵ_{eff}) is a good approximation to the actual mean field in the particle [*Polder and van Santern*, 1946]. Given the nature of this approximation, it is reasonable that the formula breaks down for a constant volume fraction as the dielectric contrast between the background and inclusion permittivities increases (Table B1); as the permittivity contrast increases, the field in the vicinity of a given particle is increasingly distorted due to neighboring particles, and the assumption of a uniform medium characterized by ϵ_{eff} surrounding the particle becomes less valid.

Although originally derived for static fields and spherical particles, it has more recently been shown that Böttcher's formula is also valid for a dense collection of randomly shaped particles, provided that the mixture is characterized by a spherical correlation function with $l \ll \lambda$, where l is the correlation length [*Tsang and Kong*, 1981, *Stogryn*, 1984].

References

Bevington, P. R., *Data Reduction and Error Analysis for the Physical Sciences*, McGraw-Hill, New York, 1969.

Böttcher, C. J. F., and P. Bordewijk, *Theory of Electric Polarization*, vol. 2, Elsevier Science, New York, 1978.

Campbell, M. J., and J. Ulrichs, Electrical properties of rocks and their significance for lunar radar observations, *J. Geophys. Res.*, *74*, 5867–5881, 1969.

Harris, D. M., and W. I. Rose, Estimating particle sizes, concentrations, and total mass of ash in volcanic clouds using weather radar, *J. of Geophys. Res.*, *88*, 10,968–10,983, 1983.

Hewlett-Packard Corporation, Measuring dielectric constant with the HP 8510 network analyzer, *Prod. Note 8510-3*, Palo Alto, Calif., 1985.

Ishimaru, A., *Electromagnetic Wave Propagation, Radiation and Scattering*, Prentice-Hall, Englewood Cliffs, N.J., 1991.

Mouginis-Mark, P., S. Rowland, P. Francis, T. Friedman, H. Garbeil J. Gradie, S. Self, L. Wilson, J. Crisp, and L. Glaze, Analysis of active volcanoes from the Earth observing system, *Remote Sens. Environ.*, *36*, 1–12, 1991.

Polder, D., and J. H. van Santern, The effective permittivity of mixtures and solids, *Physica*, *12*, 257–271, 1946.

Rose, W. I., and A. B. Kostinski, Radar remote sensing of volcanic clouds, in *Proceedings of the First International Symposium on Volcanic Ash and Aviation Safety*, edited by T. Casadevall, *U.S. Geol. Surv. Bull. 2047*, 391–396, 1994.

Stogryn, A., The bilocal approximation for the effective dielectric constant of an isotropic random medium, *IEEE Trans. Antennas Propag.*, *AP-32*(5), 517–520, 1984.

Taylor, L., Dielectric properties of mixtures, *IEEE Trans. Antennas Propag.*, *AP-13*(6), 943–947, 1965.

Tsang, L., and J. A. Kong, Scattering of electromagnetic waves from random media with strong permittivity fluctations, *Radio Sci.*, *16*(3), 303–320, 1981.

Ulaby, F. T., R. K. Moore, and A. K. Fung, *Microwave Remote Sensing*, vol. 3, Artech House, Dedham, Mass., 1986.

van Beek, L. K. H., Dielectric behavior of heterogenous systems, in *Progress in Dielectrics*, edited by J. B. Birks, pp. 69-114, CRC Press, Cleveland, Ohio, 1967.

von Hippel, A. (Ed.), *Dielectric Materials and Applications*, chap. V, pp. 291–429, MIT Press, Cambridge, Mass., 1954.

Westphal, W. B., Dielectric measuring techniques: Distributed circuits, in *Dielectric Materials and Applications*, edited by A. von Hippel, pp. 63-122, MIT Press, Cambridge, Mass., 1954.

Wolfram, S., *Mathematica: A System for Doing Mathematics by Computer*, Addison Wesley, Reading, Mass., 1989.

This preprint was prepared with the AGU LaTeX macros v3.1. File diel8 formatted 1997 March 13.

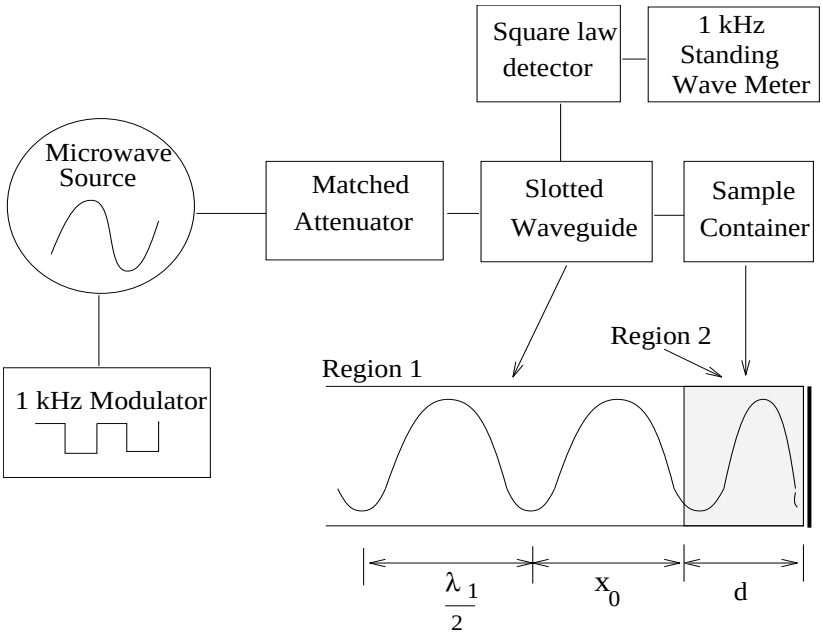

Figure 1. Experimental setup using a shorted waveguide for measuring the dielectric constant of the volcanic samples.

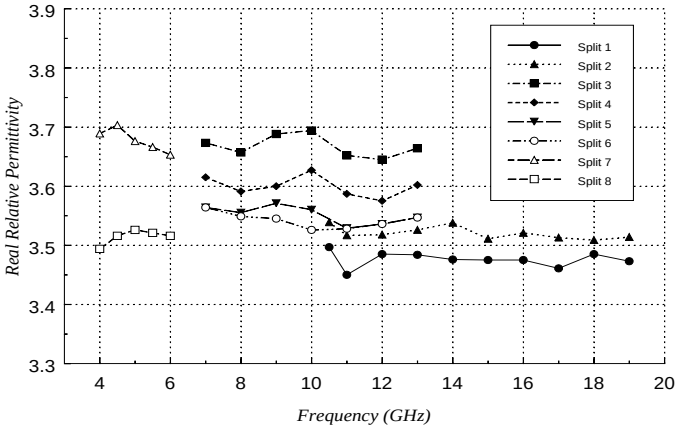

Figure 2. Real part of the complex dielectric constant versus frequency for the eight splits of the VF74-148 sample.

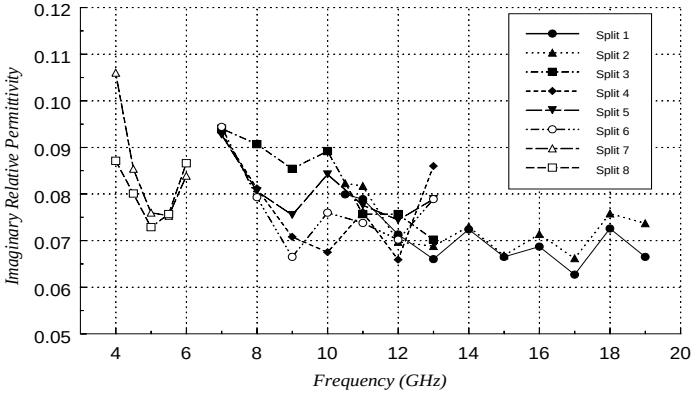

Figure 3. Imaginary part of the complex dielectric constant versus frequency for the eight splits of the VF74-148 sample.

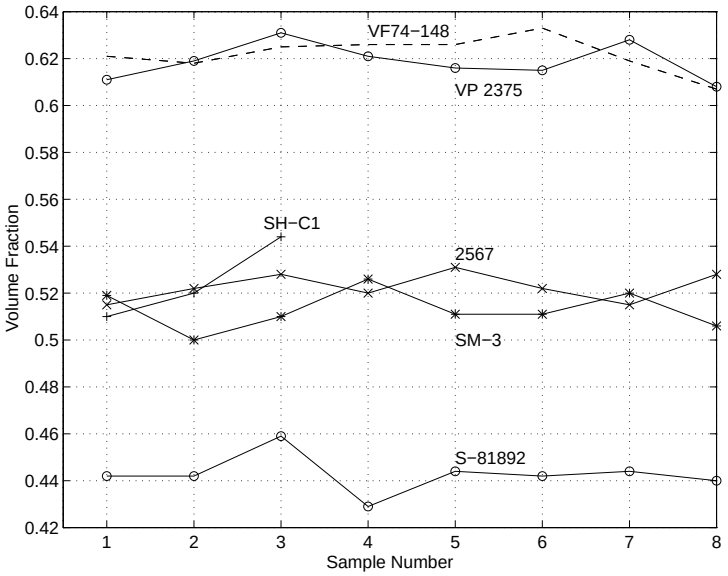

Figure 4. Volume fraction versus specimen number for the six samples listed in Table 1.

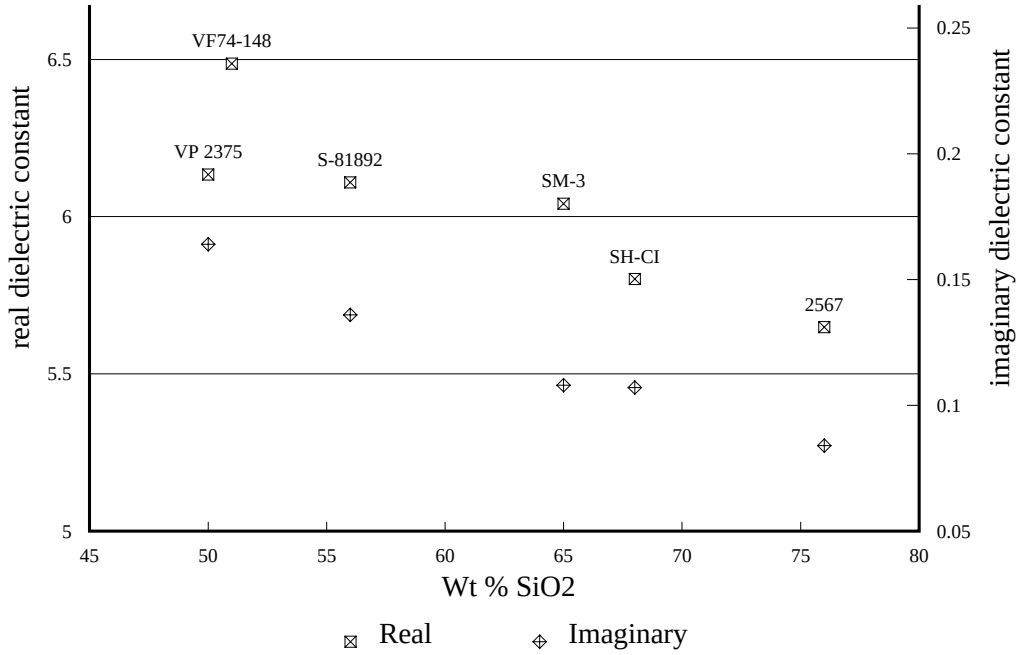

Figure 5. Real and imaginary parts of the complex permittivity of volcanic ash samples, as a function of percent SiO_2.

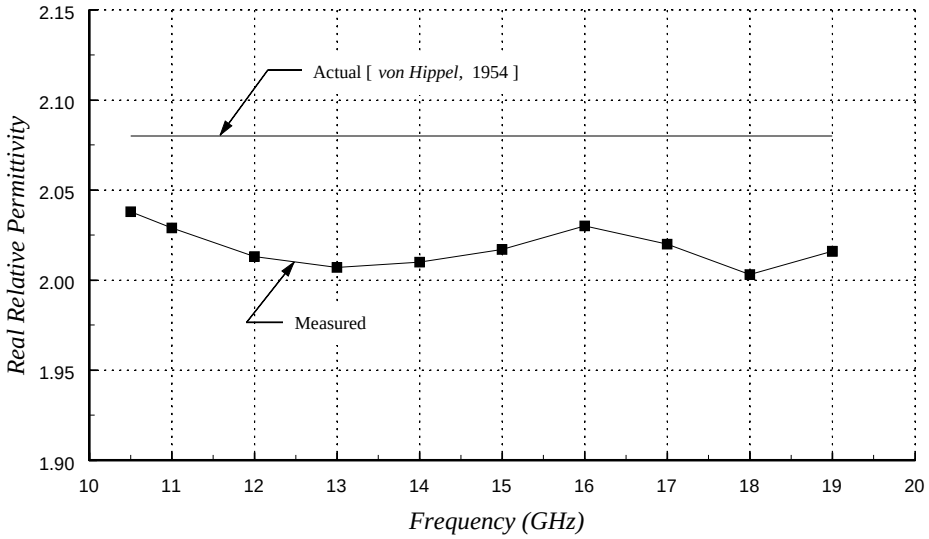

Figure A1. Measured variation in the real part of the permittivity of Teflon in the Ku - band.

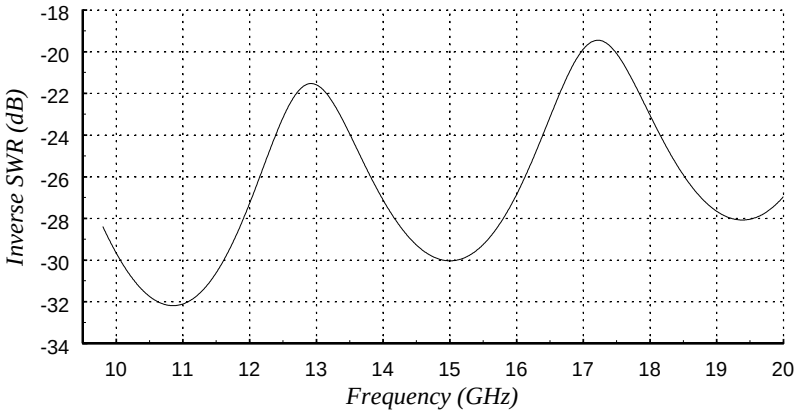

Figure A2. Inverse standing - wave - ratio versus frequency over the Ku - band with $\epsilon_2 = 3.0 - j0.03$

Table 1. Volcanic Ash Samples Studied in This Work

Sample	Volcano	Date	Composition	SiO_2, wt %	N*
VF74-148	Fuego, Guatemala	1974	basalt	51	2,4,2
VP 2375	Pacaya, Guatemala	1975	basalt	50	2,4,2
S-81892	Crater Peak/Spurr, Alaska	1992	andesite	56	2,4,2
SM-3	Santa María, Guatemala	1902	dacite	65	2,4,2
SH-CI	Mount St. Helens, Washington	1980	dacite	68	1,1,1
2567	Atitlán, Guatemala	75 ka	rhyolite	76	2,4,2

Together the samples represent the mainstream variability of volcanic ashes on Earth.
*Number of sample splits in the 10.5-19 GHz, 7-13 GHz, and 4-6 GHz ranges, respectively. These ranges roughly correspond to the IEEE band designations of Ku -, X -, and C - bands, respectively.

Table 2. Mean and Standard Deviation for the Real and Imaginary Parts of the Complex Dielectric Constants, and the Mean for the Real and Imaginary Parts of the Effective Permittivity of the Solid Ash Equivalent, for the Six Volcanic Ash Samples Studied

Sample	$< \epsilon' >$	$< \epsilon'' >$	s.d.(ϵ')	s.d.(ϵ'')	$< \epsilon'_{\rm eff} >$	$< \epsilon''_{\rm eff} >$
VF74-148	3.736	0.1229	0.0588	0.0080	6.487	0.268
VP 2375	3.561	0.0751	0.0564	0.0058	6.134	0.164
S-81892	2.542	0.0333	0.0284	0.0050	6.109	0.136
SM-3	2.900	0.0350	0.0350	0.0092	6.041	0.108
SH-CI	2.886	0.0367	0.0791	0.0038	5.802	0.107
2567	2.823	0.0287	0.0221	0.0024	5.649	0.084

Table 3. Mean and Standard Deviation for the Volume Fraction of the Six Volcanic Ash Samples Studied

Sample	Mean for f_v	s.d. for f_v
VF74-148	0.621	0.0081
VP 2375	0.619	0.0077
S-81892	0.443	0.0083
SM-3	0.513	0.0081
SH-CI	0.525	0.0170
2567	0.523	0.0061

Table A1. Fractional Variation ×100 of Measured ϵ_2' in Each of the Frequency Bands

Sample	C - band	X - band	Ku - band
VF74-148	1.4, 0.91	0.65, 1.2, 1.1, 1.2	1.0, 0.85
VP 2375	1.6, 0.67	2.4, 1.6, 1.9, 1.8	2.2, 1.4
S-81892	2.1, 1.7	3.8, 3.2, 2.2, 3.34	0.7, 1.6
SM-3	1.5, 1.5	0.94, 0.90 1.4, 1.2	1.5, 1.7
SH-C1	1.3	1.2	1.4, 4.2
2567	1.4, 1.5	0.98, 1.1, 0.83, 1.7	1.5, 0.75

Table A2. Fractional Variation ×100 of Measured ϵ_2'' in Each of the Frequency Bands (Using All Data)

Sample	C - band	X - band	Ku - band
VF74-148	13, 18	24, 27, 12, 17	14, 15
VP 2375	11, 12	15, 10, 7.7, 14	12, 18
S-81892	22, 25	35, 46, 28, 44	28, 21
SM-3	34, 12	48, 27, 26, 39	40, 50
SH-C1	7.7	28	47
2567	53, 20	17, 19, 30, 33	33, 14

Table A3. Fractional Variation ×100 of Measured ϵ_2'' in Each of the Frequency Bands (Using Data for Which $E_r > -25$ dB)

Sample	C - band	X - band	Ku - band
Sample	C-band	X-band	Ku-band
VF74-148	13, 18	7.6, 27, 5.8, 12	14, 15
VP 2375	9.9, 12	15, 10, 7.7, 14	12, 18
S-81892	1.4, 4.8	3.4, 20, 0, 1.6	14, 21
SM-3	10.4, 7.6	48, 17, 21, 19	40, 32
SH-C1	7.7	6.9	35
2567	0, 0	7.4, 6.8, 12, 13	15, 9

Table B1. Evaluation of Mixing Formulae for Three Samples

	Granite	Basalt(1)	Basalt(2) (Amygdaloidal)
Density, (g/cm^3)	2.7	3.3	3.1
Relative permittivity (solid)	$5.2 - j0.07$	$10.5 - j1.5$	$8.9 - j1.3$
Relative permittivity (powder)	$2.86 - j0.15$	$4.08 - j0.15$	$4.12 - j0.18$
Volume fraction (f_v)	0.569	0.570	0.598
Böttcher	$5.14 - j0.062$	$7.90 - j0.37$	$7.74 - j0.43$
Looyenga	$5.24 - j0.066$	$8.26 - j0.41$	$8.10 - j0.47$
Rayleigh [*Campbell and Ulrichs*, 1969]	$7.16 - j0.16$	$19.9 - j3.4$	$17.9 - j3.3$
Rayleigh (complete)	$6.52 - j0.12$	$14.0 - j1.5$	$12.8 - j1.5$
Rayleigh (higher order)	$5.75 - j0.086$	$9.66 - j0.62$	$9.00 - j0.62$